研究成果の刊行に関する一覧表

書籍：なし

論文：

1．Takahashi M, Nitta N, Kishimoto T, Ohtsuka Y, Honda S, Ashizawa K
Computed tomography findings of arc-welders' pneumoconiosis: Comparison with silicosis. Eur J Radiol 2018; 107: 98-104.

2．日野 公貴，松廣 幹雄，鈴木 秀宣，河田 佳樹，仁木 登，加藤 勝也，岸本 卓巳，芦澤 和人：３次元CT画像を用いたじん肺の重症度診断基準の定量的評価，第37回日本医用画像工学会大会，OP13-2, 2018. 7.

3．日野 公貴，松廣 幹雄，鈴木 秀宣，河田 佳樹，仁木 登，加藤 勝也，岸本 卓巳，芦澤 和人：３次元CT画像を用いたじん肺の重症度診断基準に関する粒状影の定量的評価，電子情報通信学会技術研究報告医用画像Vol. 118, No. 286, pp. 13-15, 2018. 11.

学会発表：

1．Takahashi M, Nitta, N, Kishimoto T, Otsuka Y Ashizawa K
CT findings for Arc-welders' pneumoconiosis: Comparison with silicosis 第77回日本医学放射線学会総会（横浜）2018. 4. 14.

2．日野 公貴，松廣 幹雄，鈴木 秀宣，河田 佳樹，仁木 登，加藤 勝也，岸本 卓巳，芦澤 和人：胸部３次元CT画像を用いたじん肺の粒状影定量的評価，第26回日本CT検診学会学術集会，2019. 2.

European Journal of Radiology 107 (2018) 98–104

Contents lists available at ScienceDirect

European Journal of Radiology

journal homepage: www.elsevier.com/locate/ejrad

Computed tomography findings of arc-welders' pneumoconiosis: Comparison with silicosis

Masashi Takahashi[a,*], Norihisa Nitta[b], Takumi Kishimoto[c], Yoshinori Ohtsuka[d], Sumihisa Honda[e], Kazuto Ashizawa[f]

[a] Dept. of Radiology, Yujin-Yamazaki Hospital, 80 Takegahana, Hikone, Shiga, 522-0044, Japan
[b] Dept. of Radiology, Shiga University of Medical Science, Japan
[c] Dept. of Respiratory Medicine, Okayama-Rosai Hospital, Japan
[d] Dept. of Internal Medicine, Hokkaido-Chuo-Rosai Hospital, Japan
[e] Dept. of Community-based Rehabilitation Sciences, Nagasaki University Graduate School of Biomedical Sciences, Japan
[f] Dept. of Clinical Oncology, Nagasaki University Graduate School of Biomedical Sciences, Japan

ARTICLE INFO

Keywords:
Arc-welders' pneumoconiosis
Silicosis
Computed tomography
Chest radiograph

ABSTRACT

Objective: Arc-welders' pneumoconiosis (AWP) is a less fibrogenic pneumoconiosis with radiographic shadows that can improve after isolation from dusty environments. Therefore, early diagnosis is important. However, the exact role of chest radiograph and computed tomography (CT) for diagnosing AWP is not fully understood. This study was performed to assess the CT appearance of AWP using semi-quantitative methods and to compare the findings with those of silicosis. The profusion of pulmonary abnormality on chest radiograph were also compared with the semi-quantitative CT score.

Materials and methods: Sixty-six patients with clinically diagnosed AWP were included and compared with 33 patients with silicosis. The CT images were interpreted according to the International Classification of HRCT for Occupational and Environmental Respiratory Diseases (ICOERD). Data on the profusion score by chest radiograph were also compared with CT score.

Results: Ill-defined centrilobular nodules, ground-glass opacity (GGO) and centrilobular branching opacity were more frequently observed ($p = 0.0031$) in AWP, whereas well-defined rounded opacity ($p < 0.0001$), progressive massive fibrosis ($p < 0.0001$), and mediastinal lymphadenopathy ($p < 0.0001$) were more frequently observed in silicosis. Regarding lung nodules, there was a high correlation between the ICOERD and CXR profusion scores in silicosis, but CXR underestimated AWP.

Conclusion: Ill-defined centrilobular nodules, GGO and centrilobular branching opacity were more frequently observed in AWP than silicosis. Because these findings are difficult to detect by chest radiograph, CT should be considered for the assessment of patients with suspected AWP.

1. Introduction

Arc-welders' pneumoconiosis (AWP) is a type of pneumoconiosis that is caused by chronic inhalation of fumes, which is mainly comprises iron oxide, during the welding procedure [1–3]. This condition was first reported in 1936 by Doig and McLaughlin who assessed 16 electric arc welders clinically and radiologically and found that 6 of them showed generalized fine mottling on both lung fields on chest radiograph; the remaining showed less marked changes [4]. Subsequent follow-up of the 15 patients for 9 years showed complete or partial resolution of the chest radiograph abnormalities after isolation from environmental exposure [5]. Therefore, iron oxide has been considered to be inert and to rarely cause fibrosis. However, several researches have demonstrated that some fibrosis can occur from exposure to the various materials in welding smoke other than iron oxide [6–11]. Welding smoke contains a mixture of several kinds of fumes and gases, such as nickel, asbestos, manganese, silica, beryllium, oxides of nitrogen and ozone, although some researchers have believed that iron oxide itself could cause fibrosis [6,9–11]. Early detection of AWP is crucial because early isolation from occupational exposure can contribute to resolve the abnormality and reduce the risk of fibrosis development.

High resolution computed tomography (HRCT) plays an important role in managing pneumoconiosis, not only in detecting the lung

* Corresponding author.
E-mail address: masashi@belle.shiga-med.ac.jp (M. Takahashi).

https://doi.org/10.1016/j.ejrad.2018.08.020
Received 25 May 2018; Received in revised form 23 July 2018; Accepted 22 August 2018

parenchymal abnormalities but also in assessing its extent and severity. This is especially applied in AWP because the chest radiograph is generally believed to have limited value in demonstrating minimal lung fibrosis. However, only few manuscripts have demonstrated the HRCT appearance of AWP [12–14], and there have been no studies that assessed the imaging difference between AWP and silicosis. This study was performed to clarify the HRCT appearance of AWP in comparison with that of silicosis using a semi-quantitative approach. The lung parenchymal profusion score on chest radiograph were compared with the semi-quantitative CT score, and their relationships were compared between AWP and silicosis.

2. Materials and methods

This study was supported by the Ministry of Health, Labor and Welfare Scientific Research Grant of Japan and was approved by the institutional review board of Nagasaki University Hospital and informed consent was waived from each subjects.

2.1. Subjects

A total of 66 arc welders who were seen at 3 institutes (i.e., Chugoku Rodo Eiseikyoukai, Okayama-Rosai Hospital, and Hokkaido-Chuo-Rosai Hospital) were analyzed. The cases who visited each institute for a regular health check for workers who had histories of fume dust exposure were consecutively collected from Jul 2014 to May 2015. All were men, with a mean age of 64.3 years (range, 49–84 years), who were exposed to dust fumes for a mean duration of 35.9 years (range, 9–55 years). All these subjects have been diagnosed at each institute as AWP based on occupational history and clinical findings. For comparison, 33 cases of silicosis were recruited from 1 institute (Okayama-Rosai Hospital). The cases who visited an institute for a regular health check for workers who had histories of silica dust exposure were consecutively collected from Oct 2014 to Jan 2015. 30 subjects were men and 3 were women with a mean age of 74.0 years (range, 58–83 years) and who were exposed to silica dust for a mean duration of 37.8 years (range, 8–48 years). In both the AWP and silicosis groups, there were 16 and 0 current smokers (mean Brinkman Index (BI): 664.0), respectively; 41 (mean BI: 764.0) and 26 (mean BI: 882.3) ex-smokers, respectively; and 9 and 7 never-smokers, respectively.

2.2. Imaging studies

All the subjects in both the AWP and silicosis groups underwent digital chest radiograph and CT for the purpose of regular health check, according to the Japanese workplace health management system. The CT machines used were Alexion TSX-032A/1J (Toshiba Medical Systems, Japan); TSX-302A/1A Aquilion PRIME (Toshiba Medical Systems, Japan); and Light Speed VCT (GE Health Care, USA). A supine helical CT acquisition was performed at full inspiration without contrast injection. Axial images were reconstructed contiguously 1- or 2-mm and 5 mm slice thickness. On thin-section CT, an algorithm with high spatial resolution was used for image reconstruction; the images were displayed with window width (1500 HU) and levels (−550 to −700 HU) that were appropriate for visualizing the pulmonary parenchyma. Posteroanterior digital chest radiographs were obtained using the following systems and technical factors: Velocity U (Fuji Film Medical, Japan): 125–135 kV, 125–200 mA, 30 msec; DR CALENO HC SQ (SE) (Fuji Film Medical, Japan): 125 kV, 100 mA, 20–60 msec; and KXO-80 G (Toshiba Medical Systems, Japan): 125 kV, 200–250 mA, 28–36 msec. CT and chest radiograph were displayed in a 3-megapixel LCD medical-grade, gray-scale monitor (Radiforce GS 320, Eizo, Japan).

2.3. Imaging analysis

a) Semi-quantitative analysis of CT findings:
Chest CT was interpreted with a semi-quantitative system using the International Classification of HRCT for Occupational and Environmental Respiratory Diseases (ICOERD), with some modifications [15,16]. The grade of each CT finding was judged based on the reference images of the ICOERD by consensus of 2 chest radiologists with experience of 34 and 28 years, respectively. The anonymized images of the AWP and silicosis cases were mixed and randomly displayed on the monitor.
The definitions of each CT finding were as follows [15,16]:
- a Well-defined rounded micronodule: less than 5 mm, well-defined margin, intralobular distribution may be variable (Grade 0–3).
- b Poorly-defined centrilobular micronodule, ground-glass opacity (GGO), or branching linear structure: less than 5 mm, ill-defined border, 2–3 mm from the lobular borders, or intralobular branching structure without normal tapering (Grade 0–3).
- c Diffuse to regional GGO: GGO extent of larger than 10 mm (Grade 0–3).
- d Large opacity: well-defined nodule larger than 10 mm (Grade 0, A–C, details will be described in the following section).
- e Honeycomb: clustered cystic air spaces, typically of comparable diameters in the order of 3–10 mm but occasionally as large as 25 mm; usually subpleural and is characterized by well-defined walls (Grade 0–3).
- f Reticulation: interlobular septal thickening and intralobular lines (Grade 0–3).
- g Emphysema, bullae: focal areas or regions of low attenuation, usually without visible walls; a rounded focal lucency or area of decreased attenuation, ≥10 mm in diameter, and bounded by a thin wall (Grade 0–3).
- h Pleural plaque, thickening, calcification: well-demarcated areas of pleural thickening, seen as elevated flat or nodular lesions that often contain calcification.
- i Mediastinal or hilar lymphadenopathy: bilateral, multiple enlargement of lymph nodes larger than 10 mm in the short axis.

The lungs were divided into a total of 6 zones, according to the following boundaries on the right and left: 1) upper (U), at the level of the arch of the aorta and above; 2) middle (M), from the arch of the aorta down to the inferior pulmonary vein; and 3) lower (L), inferior pulmonary vein and below, including the diaphragm. The CT findings in each zone were assessed to obtain the cumulative score for grading. The semi-quantitative scores were compared between AWP and silicosis.

b) Assessment of lung profusion abnormality by chest radiograph.
Chest radiograph was assessed in accordance with the Pneumoconiosis Law Classification System of Japan [17]. In this system, the radiographic findings of the chest were classified as either 1 of the 7 profusion (PR) categories (i.e., PR 0, 1, 2, 3, 4A, 4B, and 4C), which was equivalent to the International Classification of Radiographs of Pneumoconioses developed by the International Labour Organization. The absence of radiographic signs of pneumoconiosis was designated as PR0, whereas the presence of pneumoconiosis abnormalities was designated as PR1 to PR4. Chest radiographs with opacities that measured up to 10 mm were categorized as PR1, PR2, or PR3, depending on the increasing profusion. Small opacity profusion was recorded on a 12-point scale from 0/− to 3/+, where 0/− indicated no abnormality in both lungs and 3/+ signified the highest concentration of small opacities. Rounded and irregular opacities were independently assessed based on these categories. Large opacities, which were defined as having > 10-mm longest diameter, were classified as PR4 and sub-categorized into A, B, or C, depending on the increasing size of the opacity; category A

for up to 50 mm, B for larger than 50 mm but less than 1/3 of one hemithorax, and C for larger than 1/3 of one hemithorax. The size of a large opacity was determined by the longest diameter of a single lesion or by the cumulative longest diameters of several large opacities, relative to the area of the upper 3rd of the right lung field. The chest radiographs were independently interpreted by 2 chest radiologists with 34 and 28 years of experience, respectively; if there was discordance, the final decision was made by consensus. The anonymized chest radiographic images of the AWP and silicosis cases were mixed and randomly displayed on the monitor. To eliminate recall bias, an interval of 1 month from the CT reading session was allotted. The chest radiograph PR category for small rounded opacity was correlated with the ICOERD score, and the correlation was compared between AWP and silicosis.

2.4. Statistical analysis

The interobserver agreement for the chest radiograph PR category was assessed by Cohen's kappa coefficient; values < 0 as no agreement, 0–0.20 as slight, 0.21–0.40 as fair, 0.41–0.60 as moderate, 0.61–0.80 as substantial, and 0.81–1 as almost perfect. The original 12-point scales by the chest radiologists were converted into 5 grades (PR 0, 1, 2, 3 and 4) for statistical analysis. Comparison of the incidence of the CT findings between AWP and silicosis was assessed by the chi-square test. The relationship between the PR and ICOERD scores was compared between AWP and silicosis using analysis of covariance (ANCOVA). In the ANCOVA model, interaction terms and PR scores for the AWP and silicosis groups were included. In these analyses, a p value < 0.05 was considered statistically significant. These statistical tests were performed using MedCalc ver.10.0.2 (Medcalc Software, Mariakerke, Belgium).

3. Results

3.1. The incidence of each computed tomography finding (Table 1 and Figs. 1 and 2)

The incidence of poorly defined centrilobular nodule/GGO or branching opacity was significantly higher in AWP than in silicosis (30/66 vs. 5/33, $p = 0.0031$). On the other hand, the incidence of well-defined rounded nodule was significantly higher in silicosis than in AWP (25/33 vs. 5/66, $p < 0.0001$). Large opacity and mediastinal or hilar lymphadenopathy with/without calcification were significantly more frequent in silicosis than in AWP (14/33 vs. 4/66, $p < 0.0001$ and 27/33 vs. 10/66, $p < 0.0001$, respectively). There was no difference between AWP and silicosis in terms of reticulation, honeycomb, diffuse GGO, emphysema, and pleural plaque. The lung distribution tended to be diffuse for poorly-defined centrilobular nodule/GGO or branching opacity and more in the upper and middle lung fields than in the lower lung field for well-defined rounded nodule both in AWP and silicosis.

Table 1
Incidence of each CT findings in the cases with AWP and silicosis.

	AWP (n = 66)	Silicosis (n = 33)	
Well defined round nodule	5	25	P < 0.0001
Poorly defined centrilobular nodule, GGO, branching opacity	30	5	P = 0.0031
Large opacity	4	14	P < 0.0001
Reticulation	17	7	P = 0.2772
Honeycomb	2	1	P = 1.000
Diffuse GGO	10	8	P = 0.2714
Emphysema	43	17	P = 0.1928
Pleural plaque	22	11	P = 1.0000
Mediastinal and hilar lymphadenopathy (with calc.)	10 (6)	27(27)	P < 0.0001

3.2. The assessment of PR by chest radiograph

The interobserver agreement on the PR categories 0, 1, 2, 3, and 4 was substantial for both round opacity ($\kappa = 0.748$, 95% CI 0.654–0.858) and irregular opacity ($\kappa = 0.776$, 95% CI 0.640–0.912). The incidence of each category is shown in Fig. 3. Large opacity was found in 5% of the AWP cases (4A, n = 2 and 4B, n = 1) and in 18% of the silicosis cases (4A, n = 6). The category for small rounded opacity was higher in silicosis than in AWP.

3.3. Correlation between chest radiograph PR and CT scores (Figs. 4 and 5)

The chest radiograph PR for small rounded opacity was almost linearly correlated with the CT scores in silicosis, but it was underestimated in AWP. ANCOVA showed borderline significance ($p = 0.077$) of these two relationships.

4. Discussion

This study revealed that 1) the incidence of ill-defined centrilobular nodule/GGO or centrilobular branching opacity was significantly higher in AWP than in silicosis; 2) the incidence of large opacity and mediastinal lymphadenopathy with/without calcification was significantly higher in silicosis than in AWP; and 3) chest radiograph had a tendency to underestimate the lung parenchymal profusion abnormality of AWP, compared with that of silicosis.

The pathological findings of AWP include the presence of pigmented macrophages in the air spaces and interstitium, close to the center of the acinus, with limited fibrosis. This low component of fibrosis may be seen as an ill-defined centrilobular opacity on CT. Akira et al. assessed the thin-section CT findings of 21 arc welders and found that the most common findings were ill-defined micronodules that were diffusely distributed in the lungs (n = 15, 71.4%) [12]. Some of the micronodules appeared as fine branching structures and tended to show centrilobular distribution [12]. These ill-defined centrilobular micronodules reflect the deposition of minute iron oxide particles along the perivascular and peribronchial lymphatic vessels [12]. Han et al. analyzed the thin-section CT findings of 85 arc welders with 3–30 years of exposure and found that the predominant CT findings were poorly-defined centrilobular micronodules (n = 30, 35.3%); branching linear structure (n = 18, 21.2%); and ground glass attenuation (n = 6, 7.1%) [13]. Our results were basically consistent with previous two studies and could confirm the consensus regarding HRCT appearances of AWP. In this study, 45.5% (30/66) of the arc welders demonstrated ill-defined centrilobular nodule/GGO or branching abnormality on CT. The slight differences in the incidence of these findings among these studies were probably due to the reversible nature of AWP. Our cohort was based on a regular health check for workers who had histories of fume dust exposure and might have included both active and inactive workers.

One differential diagnosis of centrilobular ill-defined opacity and branching opacity on thin-section CT is respiratory bronchiolitis [13], which is similar to AWP in terms of the pathological findings of inflammatory cell infiltration, which is often accompanied by pigment, in the walls of the membranous and respiratory bronchioles and alveolar ducts. Han et al. revealed that centrilobular ill-defined opacity on thin-section CT was much frequently observed in AWP than in smokers [13]. In that study, the high percentage of smokers in the AWP cases might cast doubt on whether the findings truly represented exposure to welding and were not the results of smoking; however, the authors suggested that the findings were mostly due to exposure to arc welding because the rates of positive thin-section CT findings in the arc welders were almost equal between smokers and non-smokers. In our present study, all cases had smoking history; therefore, the influence of smoking on the thin-section CT findings cannot be excluded. To solve this issue,

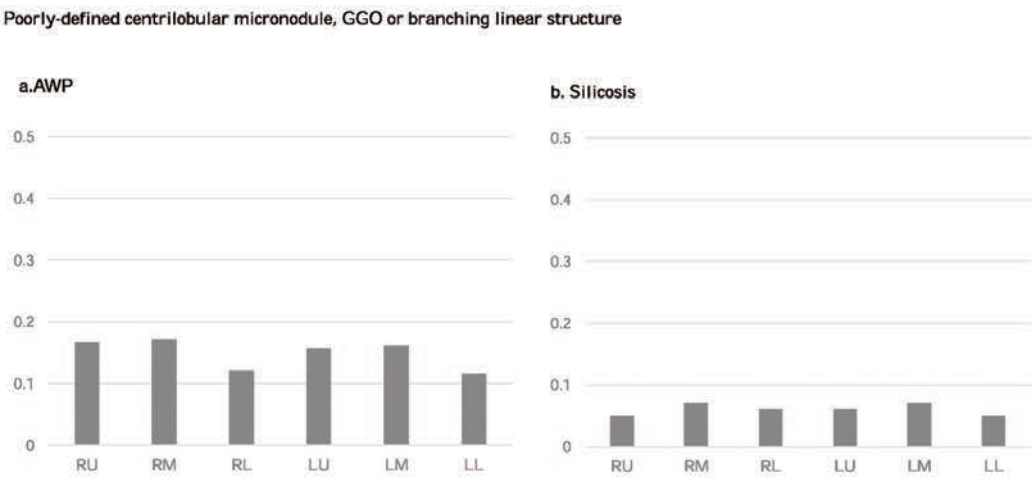

Fig. 1. Comparison of the CT score and the distribution of poorly-defined centrilobular micronodules, GGO, and branching linear structures within the lungs between AWP (a) and silicosis (b). The height of each bar represents the average score for each lung zone. The lung distribution tended to be diffuse for poorly-defined centrilobular nodule/GGO or branching opacity both in AWP and silicosis.

the CT findings should be compared between AWP and smokers, as performed by Han et al. [13].

Mixed dust pneumoconiosis (MDP) is another differential diagnosis. MDP is a less fibrotic pneumoconiosis in the presence of low silica content [18]. Hyalinization which is a hallmark for silicosis is not observed in MDP and infiltrative fibrosis is found in the surrounding interstitium [18]. Therefore chest radiograph shows ill-defined nodules and CT shows irregular shaped nodular opacity [18]. Usually mixed dust fibrosis and silicotic nodules are coexisted in the lung field and diffusely distributed ill-defined centrilobular nodule/GGO or branching abnormality as observed in AWP is not demonstrated. Information regarding typical occupations associated with a diagnosis of MDP include metal miners, quarry workers, foundry workers, pottery and ceramic workers, and stonemasons is also helpful for making a diagnosis of MDP [18].

Silicotic nodules tend to conglomerate and form a > 1-cm large opacity, which is consistent with progressive massive fibrosis [19]. Additionally, hilar and mediastinal lymphadenopathy with calcification is a radiologic hallmark of silicosis [19,20]. This study has demonstrated that the incidences of both large opacity and lymphadenopathy were significantly lower in AWP than in silicosis. Many researchers have believed that large opacity and lymphadenopathy are due to the strong fibrogenic property of inhaled silica [19]. Silica-exposed macrophages release fibroblast growth factor that facilitates the accumulation of fibroblasts and fibroblast products, which, in turn, induce inflammatory and fibrogenic reactions in the interstitium, alveoli, and lymph node [20]. These fibrogenic reactions lead to the formation of interstitial silicotic nodules that tend to conglomerate. Additionally, the free-particulate silica that is not ingested by macrophages can enter the perivascular lymphatic channels to be translocated to the draining mediastinal lymph nodes and cause fibrosis [20]. On the other hand, iron oxide itself is considered an inert material and has a low potential to cause fibrosis in both the lung and lymph node. The low incidence of large opacity and lymphadenopathy in the imaging of AWP probably reflected this pathological background. Attfield et al. analyzed the chest radiograph of 661 British electric arc welders and found no case with large opacity [21].

Thus AWP have been believed not develop fibrosis both in the lung field and lymphnode, some researchers found that AWP can be associated with fibrosis [6–11]. Akira et al. found that 3 of 21 arc welders

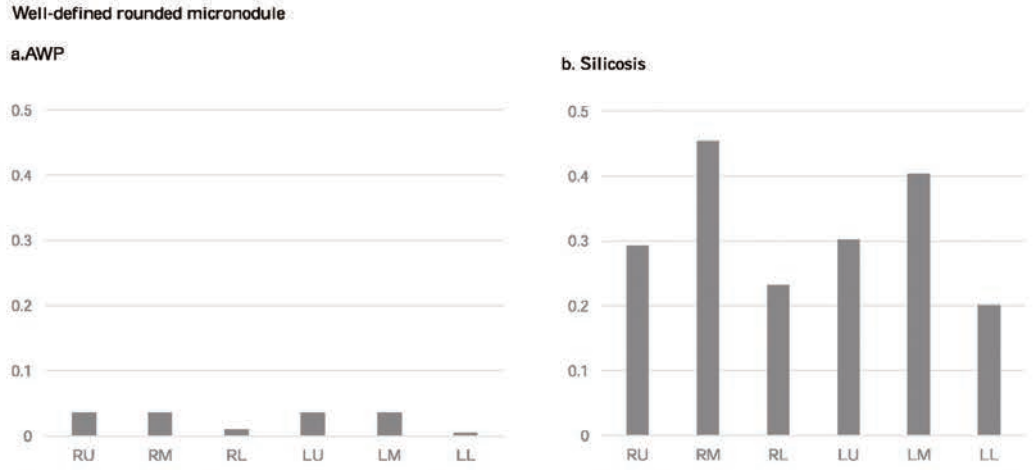

Fig. 2. Comparison of the CT score and the distribution of well-defined rounded micronodules within the lungs between AWP (a) and silicosis (b). The height of each bar represents the average score for each lung zone. The lung distribution tended to be more in the upper and middle lung fields than in the lower lung field for well-defined rounded nodule both in AWP and silicosis.

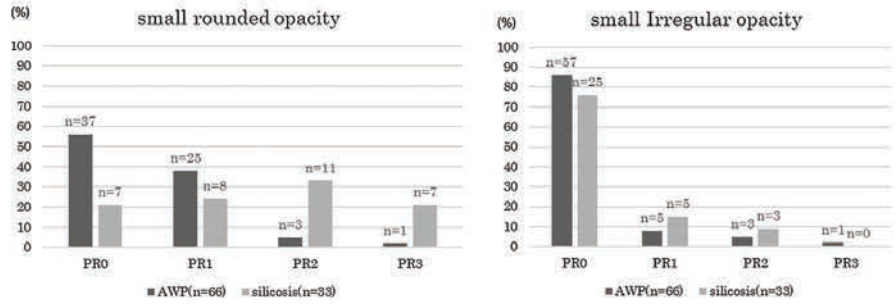

Fig. 3. The incidence of chest radiograph profusion for small rounded opacity and irregular opacity. The large opacity (PR4) was excluded. The category for small rounded opacity was higher in silicosis than in AWP.

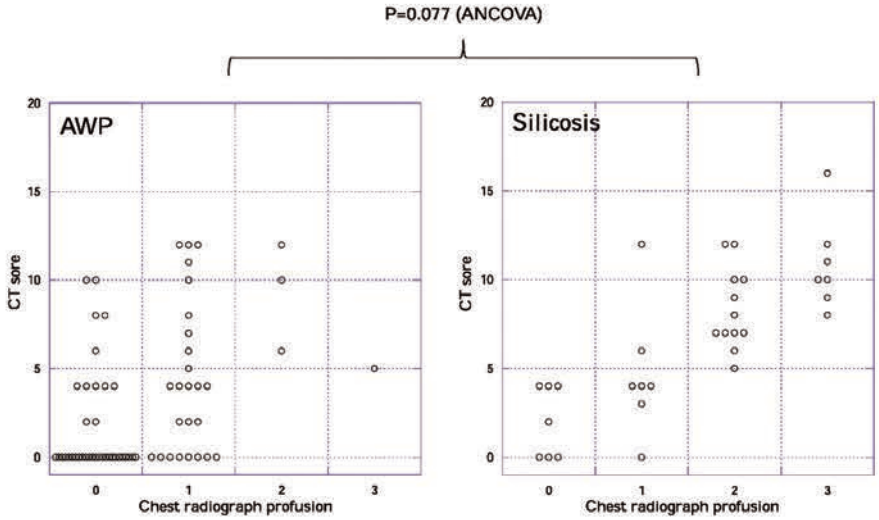

Fig. 4. Relationship between chest radiograph profusion and CT score in cases with AWP and silicosis.
Although there is an almost linear correlation between the chest radiograph profusion and CT scores in silicosis, the chest radiograph profusion score was underestimated in AWP. Analysis of covariance revealed borderline significance of these 2 relationships ($p = 0.077$).

showed a pulmonary conglomerate mass on CT [12]. The fibrosis in AWP is suspected to develop from concomitant exposure to irritants, such as asbestos and silica [12]. Although the number of cases was small, this study demonstrated that some AWP cases had large opacity (4/66, 6.0%) and lymphadenopathy (10/66, 15.2%) on CT. Probably, in these workers, the inhaled fumes contained some fibrogenic irritants other than iron oxide.

The Ministry of Health, Labor and Welfare of Japan has established the Pneumoconiosis Law in 1960 to protect the health and promote the welfare of dust-exposed workers [17]. This law indicated the use of chest radiograph to assess and classify the severity of pneumoconiosis, and CT can be used only as a reference. However, this present study demonstrated that chest radiograph had a tendency to underestimate the detection of lung abnormalities of AWP, in comparison with silicosis. This result may account for the less fibrogenic features of the lung nodule in AWP. To avoid overlooking the presence of AWP, the use of CT should be considered if a detailed work history on arc welding is obtained early. Although most of the lung abnormalities of AWP were reversible, some cases developed lung fibrosis. Therefore, early detection of AWP is extremely important to prevent the development of fibrosis and to protect the health of arc welders.

This study had some limitations. First, in this cohort, pathological proof was not obtained and the diagnosis of AWP was established only by clinical findings and occupational history. As described above, the possibility of disorders other than AWP, such as smoking-related diseases, could not be confidently excluded because almost all of the workers in this study were smokers. Second, the imaging protocol for the workers was not fixed because the cohort was recruited from 3 different institutes. Therefore, the different technical factors of CT scan might have influenced the incidence of each CT finding. Third, although the ICOERD was used with some modification for semi-quantitative analysis, it did not contain enough imaging references, especially for ill-defined centrilobular nodules/GGO or branching opacity. Therefore, subjective bias on the grading for each CT finding cannot be completely excluded.

In conclusion, ill-defined centrilobular nodules/GGO and centrilobular branching opacity were more frequently observed in AWP, whereas well-defined rounded opacity, large opacity, and mediastinal lymphadenopathy were more frequently observed in silicosis. Regarding lung nodules, there was a high correlation between the CT score and the chest radiograph PR for silicosis, but the chest radiograph underestimated AWP. Therefore, in patients with suspected AWP, CT should be considered for the detection of early-stage disease before progression to fibrosis.

Author declaration

We confirm that the manuscript has been read and approved by all named authors and that there are no other persons who satisfied the criteria for authorship but are not listed. We further confirm that the order of authors listed in the manuscript has been approved by all of us. We confirm that we have given due consideration to the protection of intellectual property associated with this work and that there are no impediments to publication, including the timing of publication, with respect to intellectual property. In so doing we confirm that we have followed the regulation of our institutions concerning intellectual property.

We further confirm that any aspect of the work covered in this

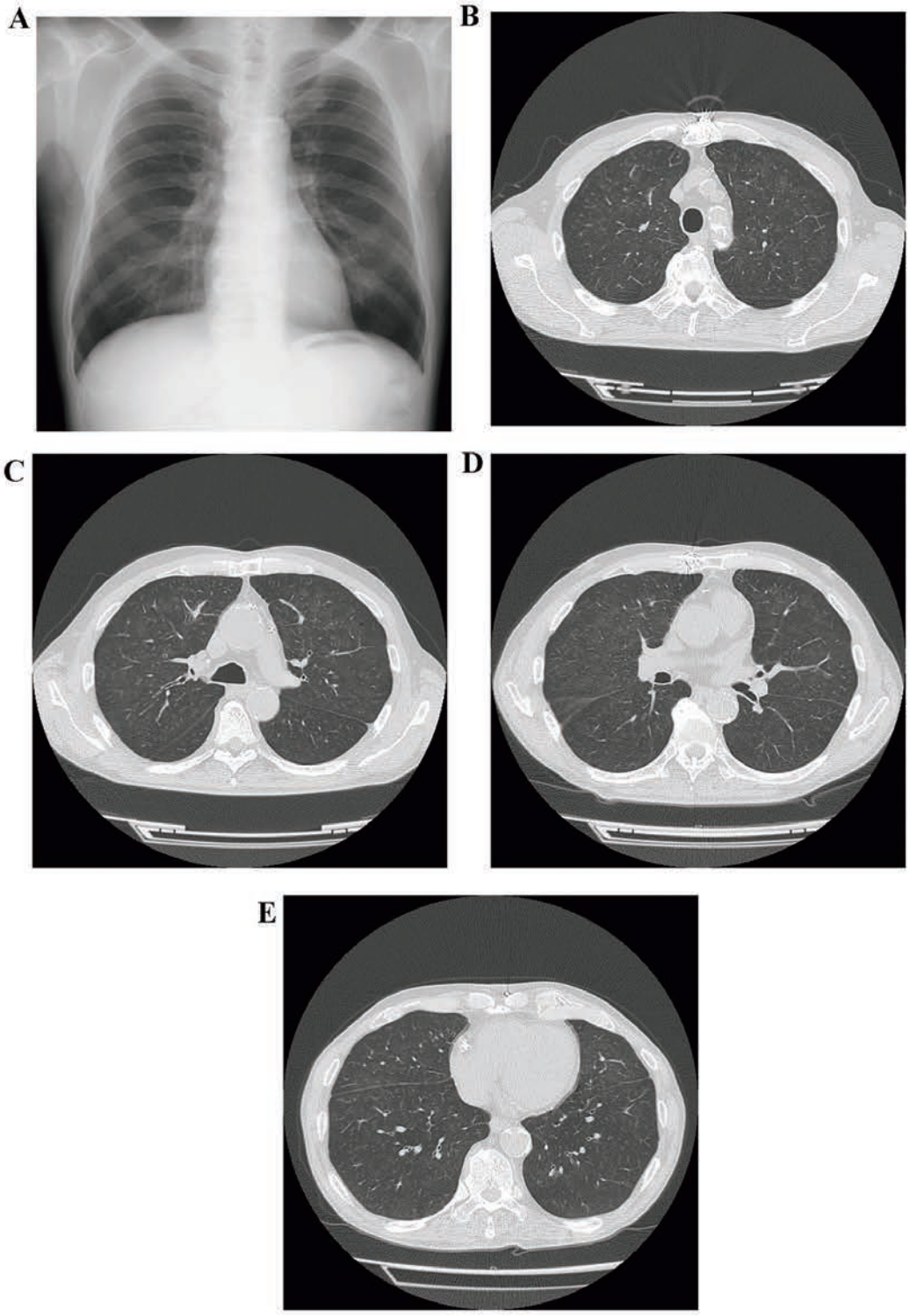

Fig. 5. Images in a 71-year-old man who was employed as an arc-welder for 55 years.
(a) Chest radiograph reveals no parenchymal abnormality and was judged by both chest radiologists to have a score of 0 for lung profusion abnormality. (b–e) Thin-section CT scans show numerous poorly defined centrilobular ground-glass nodules that are diffusely distributed throughout the lung. The ICOERD score for poorly-defined centrilobular micronodule, GGO, or branching linear structure in this case is 10 (full score is 18).

manuscript that has involved either experimental animals or human patients has been conducted with the ethical approval of all relevant bodies and that such approvals are acknowledged within the manuscript.

Acknowledgement

This study was supported by the Ministry of Health, Labor and Welfare Scientific Research Grant of Japan.

References

[1] S.J. Sferlazza, W.S. Beckett, The respiratory health of welders, Am. Rev. Respir. Dis. 143 (5 Pt. 1) (1991) 1134–1148.
[2] J.M. Antonini, Health effects of welding, Crit. Rev. Toxicol. 33 (1) (2003) 61–103.
[3] C.G. Billings, P. Howard, Occupational siderosis and welders' lung: a review, Monaldi Arch. Chest Dis. 48 (4) (1993) 304–314.
[4] A. Doig, A. McLaughlin, X ray appearances of the lungs of electric arc welders, Lancet 1 (4) (1936) 771–775.
[5] A. Doig, A. McLaughlin, Clearing of X-ray shadows in welders' siderosis, Lancet 1 (6508) (1948) 789–791.
[6] A. Funahashi, D.P. Schlueter, K. Pintar, E.L. Bemis, K.A. Siegesmund, Welders' pneumoconiosis: tissue elemental microanalysis by energy dispersive x ray analysis, Br. J. Ind. Med. 45 (1) (1988) 14–18.
[7] W.K. Morgan, Arc-welders' lung complicated by conglomeration, Am. Rev. Respir. Dis. 85 (1962) 570–575.
[8] T.L. Guidotti, J.L. Abraham, P.B. DeNee, J.R. Smith, Arc Welders' pneumoconiosis: application of advanced scanning electron microscopy, Arch. Environ. Health 33 (3) (1978) 117–124.
[9] R. Charr, Respiratory disorders among welders, Am. Rev. Tuberc. 71 (6) (1955) 877–884.
[10] R. Charr, Pulmonary changes in welders: a report of three cases, Ann. Intern. Med. 44 (4) (1956) 806–812.
[11] E.C. Meyer, S.F. Kratzinger, W.H. Miller, Pulmonary fibrosis in an arc welder, Arch. Environ. Health 15 (4) (1967) 462–469.
[12] M. Akira, Uncommon pneumoconioses: CT and pathologic findings, Radiology 197 (2) (1995) 403–409.
[13] D. Han, J.M. Goo, J.G. Im, K.S. Lee, D.M. Paek, S.H. Park, Thin-section CT findings of arc-welders' pneumoconiosis, Korean J. Radiol. 1 (2) (2000) 79–83.
[14] C. Yoshii, T. Matsuyama, A. Takazawa, et al., Welder's pneumoconiosis: diagnostic usefulness of high-resolution computed tomography and ferritin determinations in bronchoalveolar lavage fluid, Intern. Med. 41 (12) (2002) 1111–1117.
[15] Y. Kusaka, K. Hering, J. Parker, International Classification of HRCT for Occupational and Environmental Respiratory Diseases, Springer-Verlag, Tokyo, 2005.
[16] K.G. Hering, K. Hofmann-Preiß, T. Kraus, Update: standardized CT/HRCT classification of occupational and environmental thoracic diseases in Germany, Radiologe 54 (4) (2014) 363–384.
[17] N.A. Jp, M. Imanaka, N. Suganuma, Japanese workplace health management in pneumoconiosis prevention, J. Occup. Health 59 (2) (2017) 91–103.
[18] K. Honma, J.L. Abraham, K. Chiyotani, et al., Proposed criteria for mixed-dust pneumoconiosis: definition, descriptions, and guidelines for pathologic diagnosis and clinical correlation, Hum. Pathol. 35 (12) (2004) 1515–1523.
[19] G.C. Ooi, K.W. Tsang, T.F. Cheung, et al., Silicosis in 76 men: qualitative and quantitative CT evaluation—clinical-radiologic correlation study, Radiology 228 (3) (2003) 816–825.
[20] C.G. Ooi, P.L. Khong, R.S. Cheng, et al., The relationship between mediastinal lymph node attenuation with parenchymal lung parameters in silicosis, Int. J. Tuberc. Lung Dis. 7 (12) (2003) 1199–1206.
[21] M.D. Attfield, D.S. Ross, Radiological abnormalities in electric-arc welders, Br. J. Ind. Med. 35 (2) (1978) 117–122.

3次元CT画像を用いた じん肺の重症度診断基準の定量的評価

日野 公貴[*1] 松廣 幹雄[*2] 鈴木 秀宣[*2] 河田 佳樹[*2] 仁木 登[*2]
加藤 勝也[*3] 岸本 卓巳[*4] 芦澤 和人[*5]

要旨

じん肺は，粉じんを肺に吸入することによって生じる職業性呼吸器疾患である．我国において毎年24万人前後の粉じん労働者がじん肺健康診断を受診している．じん肺診断では胸部単純X線写真を用いているが近年ではCT画像を用いた定量的な診断法が検討されている。本報告では，じん肺CT画像の第0型0/1，第1型1/0，第1型1/1，第1型1/2，第2型2/2から2回のマニュアル処理と自動処理で粒状影を抽出し．じん肺CT画像データベースを作成する．このデータベースを用いてX線写真の診断結果と粒状影の個数・大きさ・重症度別に解析・比較・評価を行う．

キーワード：CT，CAD，医用画像処理

1. はじめに

じん肺は，粉じんを肺に吸入することによって生じる職業性呼吸器疾患である。日本の粉じん作業従事労働者数は昭和 60 年をピークに減少し，平成12年で35万人であったが，近年は約 50 万人前後で推移しており増加傾向となっている．じん肺が進行すると肺結核・続発性気胸・肺がんなどの合併症に罹患しやすくなるため，健康診断で適切な診断・治療が必要である．

また，じん肺健康診断として胸部単純X線撮影や肺機能検査が実施されている．胸部単純X線写真によって第0型，第1型，第2型，第3型，第4型に分類され，第1型以上の患者は労災認定となるが第0型の患者は労災認定の対象とならないため正確に診断しなければならない．ここで，近年では胸部CT検査による定量的な診断法が検討されている．本報告では，じん肺CT画像の第0型0/1，第1型1/0，第1型1/1，第1型1/2，第2型2/2から2回のマニュアル処理と自動処理で粒状影を抽出し．じん肺CT画像データベースを作成する．このデータベースを用いてX線写真の診断結果と粒状影の個数・大きさ・重症度別に解析・比較・評価を行う．

*1 徳島大学大学院先端技術科学教育部
〔〒770-8502 徳島県徳島市南常三島町 2-1〕
e-mail: c501738006@tokushima-u.ac.jp
*2 徳島大学大学院社会産業理工学研究部
*3 川崎医科大学
*4 岡山ろうさい病院
*5 長崎大学

2. 撮影条件と手法

岡山ろうさい病院で診断されたじん肺 25 症例(0/1 - 5 例，1/0 - 5 例，1/1 - 5 例，1/2 - 5 例，2/2 - 5 例)を用いた．撮影条件を表1に示し，症例別の職業歴を表2に示す．これらのCT 画像に(1)粒状影のマニュアル抽出，(2) CAD を用いた結節の自動抽出，(3)粒状影の定量評価を適用した．

表 1　撮影条件

装置	Aquilion PRIME
管電圧[kV]	120
管電流[mA]	240
スライス厚[mm]	1.0
画素間隔[mm]	0.625 , 0.781
再構成間隔[mm]	1.0
再構成関数	FC13-H,FC52

表 2　型区分と職業歴

病型区分	職業歴
第 0 型　0/1	窯業　3 症例 船舶製造業　1 症例 随道掘削　1 症例
第 1 型　1/0	窯業　5 症例
第 1 型　1/1	建設業　2 症例 採石業　2 症例 船舶製造業　1 症例
第 1 型　1/2	窯業　3 症例 セメント製造業　1 症例 採石業　1 症例
第 2 型　2/2	採石業　4 症例 採鉱業　1 症例

(1) 粒状影のマニュアル抽出

粒状影のマニュアル抽出は，WL500，WW1500 で設定し Axial 面で抽出する．右肺尖部，右肺底部，左肺尖部，左肺底部の順で抽出し，抽出は 2 回行い 1 回目と 2 回目の読影間隔は半年以上と 1 週間を置いた．1 回目と 2 回目の論理和をマニュアル抽出結果とする．

(2) CAD を用いた結節の自動抽出

本研究室で開発されている CAD の結節自動抽出結果とマニュアル抽出結果を重ね合わせ新たに見直し，未抽出の粒状影があればじん肺 CT 画像データベースに追加する．

(3) 粒状影の定量評価

粒状影が球であると仮定して，粒状影の大きさは体積から求められる直径で定義する．そして，じん肺の重症度を粒状影の個数，大きさ，体積によって評価する．

3. 結果

第 0 型 0/1 と第 1 型 1/0 の粒状影の抽出結果例を図 1 に示す．粒状影数を見ると診断結果と一致しない症例があった．図 2 に粒状影の直径と累積頻度の関係を示す．重症度に関わらず直径 3mm 以上の粒状影では指数関数的に数が増加しているが 3mm 以下になると緩やかになる傾向が見られた．

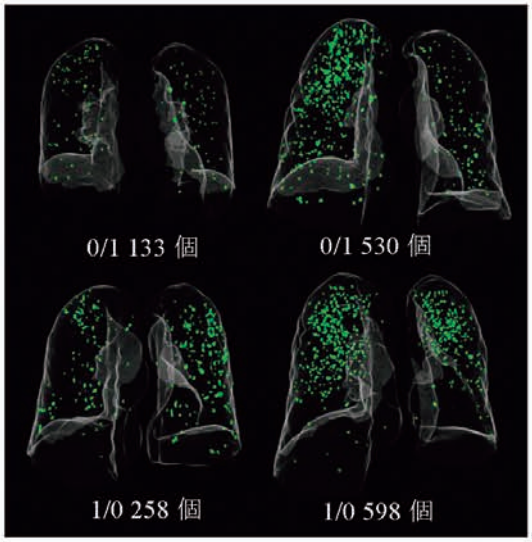

図 1　粒状影の抽出結果

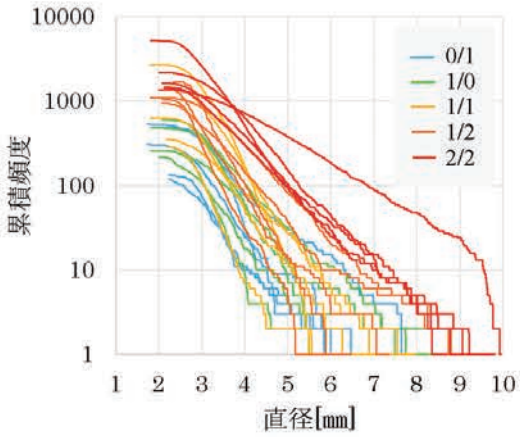

図 2　粒状影の直径と累積頻度

図 3 に X 線写真によって第 0 型 0/1，第 1 型 1/0 と診断された症例と CT 画像による定量評価結果（粒状影数）に基づいて第 0 型 0/1（CT），第 1 型 1/0（CT）と診断された症例について重症度別で平均粒状影数と標準偏差を求めた結果を示す．また，Mann-Whitney U 検定をそれぞれの診断結果に対して行った結果 X 線写真の診断結果では有意差はみられなかったが，CT 画像の定量評価結果に基づく診断結果では有意差が認められた．

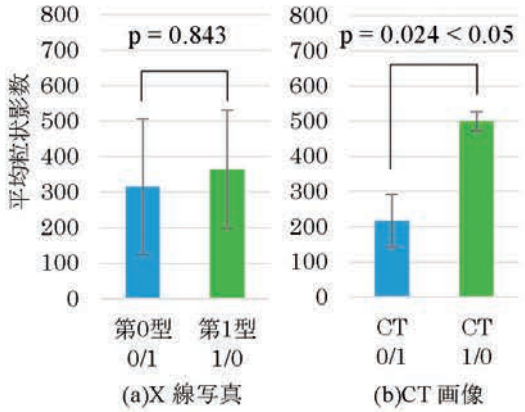

図 3　X 線写真の診断結果と CT 画像を用いた診断結果の評価

4. まとめ

じん肺 CT 画像から粒状影を抽出し，粒状影の定量評価を行った．CT 画像を用いた定量評価結果を提示することにより，より正確にじん肺の重症度を分類することが可能となり，診断精度の向上が期待できる．今後の課題として多症例に適用し，より正確なじん肺 CT 画像データベースの作成と高精度な粒状影自動抽出法について検討する．

利益相反の有無

なし

文　献

[1] H. Suzuki, Y. Kawata, N. Niki, et al: Computer aided diagnosis for severity assessment of pneumoconiosis using CT images, Proc. SPIE Medical Imaging, Vol.9785, pp.978531-1-6, 2016.

[2] K. Kanazawa, Y. Kawata, N. Niki, et al: Computer-aided diagnosis for pulmonary nodules based on helical CT images, Comput. Med. Imag. Graphics, vol. 22, no. 2, pp. 157–167, 1998.

[3] Y. Kawata, N. Niki, H. Ohmatsu, et al: Quantitative classification based on CT histogram analysis of non-small cell lung cancer: Correlation with histopathological characteristics and recurrence-free survival, Medical Physics, vol.39, no.2, pp.988-1000, 2012.

[4] 松廣幹雄，鈴木秀宣，河田佳樹，他：胸部マルチスライス CT 画像における葉間裂抽出法，電子情報通信学会論文誌，Vol.J.96-D，no.4，pp.834-843，April，2013.

[5] 滝島任，中村雅夫，千代谷慶三：じん肺患者の呼吸機能検査ハンドブック．真興交易医書出版部，1991，P3-10

[6] 永井厚志編：呼吸器疾患　第 3 版．日本医事新報社，2015，P241-250

[7] K. Hino, M. Matsuhiro, H. Suzuki, et al: Quantitative assessment for pneumoconiosis severity diagnosis using 3D CT images, Proc. SPIE Medical Imaging, Vol.10575, pp.105753J-1-6, 2018.

Quantitative assessment for pneumoconiosis severity diagnosis using 3D CT images

Koki Hino[*1], Mikio Matsuhiro[*2], Hidenobu Suzuki[*2],Yoshiki Kawata[*2],Noboru Niki[*2]
Katsuya Kato[*3], Takumi Kishimoto[*4], Kazuto Ashizawa[*5]

*1 System Innovation Engineering Graduate School of Advanced Technology and Science The University of Tokushima
*2 Tokushima University
*3 Kawasaki Medical School
*4 Okayama Rosai Hospital
*5 Nagasaki University

Pneumoconiosis is an occupational respiratory illness that occur by inhaling dust to the lungs. 240,000 participants are screened for diagnosis of pneumoconiosis every year in Japan. Radiograph is used for staging of severity rate in pneumoconiosis worldwide. CT imaging is useful for the differentiation of requirements for industrial accident approval because it can detect small lesions in comparison with radiograph. In this paper, we extracted lung nodules from 3D pneumoconiosis CT images by two manual processes and automatic process, and created a database of pneumoconiosis CT images. We used the database to analyze, compare, and evaluate visual diagnostic results of radiographs and quantitative assessment (number, size and volume) of lung nodules. This method was applied to twenty five pneumoconiosis patients. Initial results showed that the proposed method can assess severity rate in pneumoconiosis quantitatively. This study demonstrates effectiveness on diagnosis and prognosis of pneumoconiosis in CT screening.

Key words: X-ray image, CT, Medical image processing

一般社団法人 電子情報通信学会
THE INSTITUTE OF ELECTRONICS,
INFORMATION AND COMMUNICATION ENGINEERS

信学技報
IEICE Technical Report

3 次元 CT 画像を用いた じん肺の重症度診断基準に関する粒状影の定量的評価

日野 公貴† 松廣 幹雄‡ 鈴木 秀宣‡ 河田 佳樹‡ 仁木 登‡
加藤 勝也†‡ 岸本 卓巳‡‡ 芦澤 和人†‡‡
†徳島大学大学院 先端技術科学教育部〒770-8502 徳島県徳島市南常三島町 2-1
‡徳島大学大学院 社会産業理工学研究部
†‡川崎医科大学
‡‡岡山ろうさい病院
†‡‡長崎大学

E-mail: †c501738006@tokushima-u.ac.jp

あらまし じん肺は，粉じんを肺に吸入することによって生じる職業性呼吸器疾患である．我国において毎年 24 万人前後の粉じん労働者がじん肺健康診断を受診している．じん肺の診断では単純 X 線写真を用いているが，近年では単純 X 線写真に比べて正確に病変を評価することができる 3 次元 CT 画像を用いた高精度な病型区分を作成することが期待されている．本研究では，3 次元 CT 画像を用いてじん肺の定量的な診断基準を作成することを目指している．このために，じん肺 CT 画像のデータベースを作成して解析し，じん肺の粒状影の個数，大きさと CT 値，分布型を用いて重症度を定量的に評価する．

キーワード CT，CAD，医用画像処理，じん肺

1. 背景・目的

じん肺は，粉じんを肺に吸入することによって生じる職業性呼吸器疾患である。日本の粉じん作業従事労働者数は昭和 60 年をピークに減少し，平成 12 年で 35 万人であったが，近年は約 50 万人前後で推移しており増加傾向となっている．じん肺が進行すると肺結核・続発性気胸・肺がんなどの合併症に罹患しやすくなるため，健康診断で適切な診断・治療が必要である．

また，じん肺健康診断として胸部単純 X 線撮影や肺機能検査が実施されている．胸部単純 X 線写真によって第 0 型，第 1 型，第 2 型，第 3 型，第 4 型に分類され，第 1 型以上の患者は労災認定となるが第 0 型の患者は労災認定の対象とならないため正確に診断しなければならない．ここで，近年では単純 X 線写真に比べて正確に病変を評価することができる 3 次元 CT 画像を用いた高精度な病型区分を作成することが期待されている．本研究では，3 次元 CT 画像を用いてじん肺の定量的な診断基準を作成することを目指している．このために，じん肺 CT 画像のデータベースを作成して解析し，じん肺の粒状影の個数，大きさと CT 値，分布型を用いて重症度を定量的に評価する．

2. 撮影条件と手法

岡山ろうさい病院で診断されたじん肺 25 症例(0/1 - 5 例，1/0 - 5 例，1/1 - 5 例，1/2 - 5 例，2/2 - 5 例)を用いた．症例別の病型区分と職業歴を表 1 に示し，撮影条件を表 2 に示す．これらの CT 画像に(1)粒状影のマニュアル抽出，(2) CAD を用いた結節の自動抽出，(3)じん肺の定量評価を適用した．

表 1 病型区分と職業歴

病型区分	職業歴
X 線 0/1	窯業 3 症例 船舶製造業 1 症例 随道掘削 1 症例
X 線 1/0	窯業 5 症例
X 線 1/1	建設業 2 症例 採石業 2 症例 船舶製造業 1 症例
X 線 1/2	窯業 3 症例 セメント製造業 1 症例 採石業 1 症例
X 線 2/2	採石業 4 症例 採鉱業 1 症例

表 2　撮影条件

装置	Aquilion PRIME
管電圧[kV]	120
管電流[mA]	240
スライス厚[mm]	1.0
画素間隔[mm]	0.625 , 0.781
再構成間隔[mm]	1.0
再構成関数	FC13-H,FC52

(1)　粒状影のマニュアル抽出

粒状影のマニュアル抽出は，WL500，WW1500 で設定し Axial 面で抽出する．右肺尖部，右肺底部，左肺尖部，左肺底部の順で抽出し，抽出は 2 回行い 1 回目と 2 回目の読影間隔は半年以上と 1 週間を置いた．1 回目と 2 回目の論理和をマニュアル抽出結果とする．

(2)　CAD を用いた結節の自動抽出

本研究室で開発されている CAD の結節自動抽出結果とマニュアル抽出結果を重ね合わせ新たに見直し，未抽出の粒状影があればじん肺 CT 画像データベースに追加する．

(3)　じん肺の定量評価

じん肺の重症度を粒状影の個数，大きさと CT 値，分布型によって評価する．

(3)－1 粒状影の個数と大きさ

粒状影の大きさは，粒状影が球であると仮定して，体積から求められる直径で定義する．

(3)－2 粒状影の分布型

粒状影を構成するピクセル群から重心点の座標を求め,各粒状影の重心点間の最短距離を算出し，その最短距離と相対度数で分布型を評価する．

3. 結果

X 線 0/1 と X 線 1/2 の粒状影の抽出結果例を図 1 に示す．

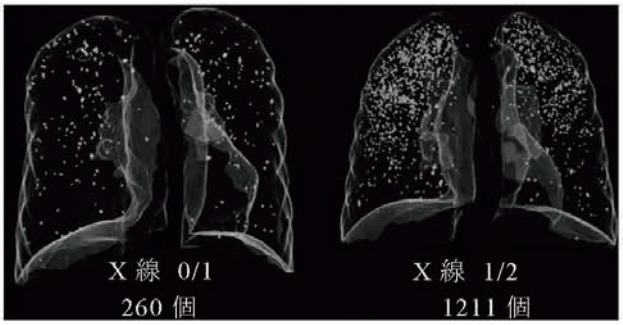

図 1　粒状影の抽出結果

図 2 に大きさ別における粒状影数の増加パターンを示す．重症度の低い症例と高い症例が混在しており診断結果と一致していない症例があり，増加パターンも様々であることが分かった．

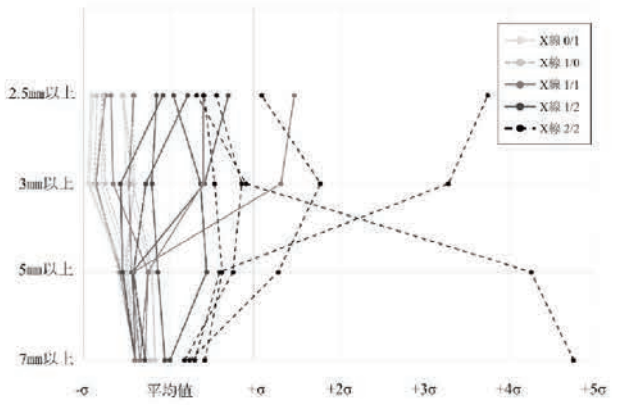

図 2　大きさ別における粒状影数の増加パターン

図 3 に肺の部位別における粒状影の個数と大きさの関係を示す．部位別では 25 症例中 18 症例が上部に粒状影がある割合が多く，左肺より右肺のほう多い傾向が見られた．

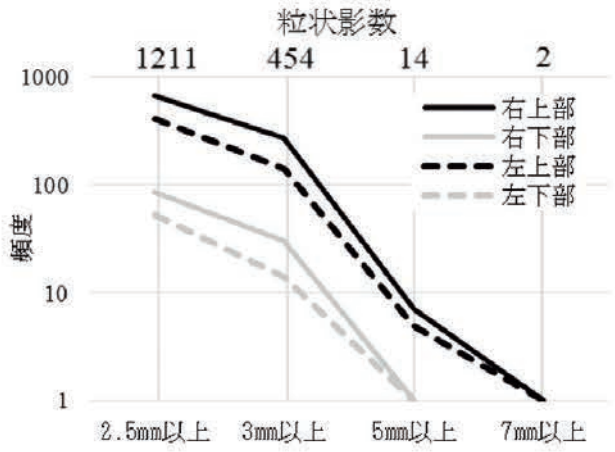

図 3　肺の部位別における粒状影の個数と大きさの関係（X 線 1/2）

図 4 に病型区分別における粒状影の大きさと平均 CT 値の関係を示す．1-5 ㎜までは，同じ大きさでも重症度別に差がある事が分かった．5 ㎜以上では，平均 CT 値にばらつきがある傾向が見られた．

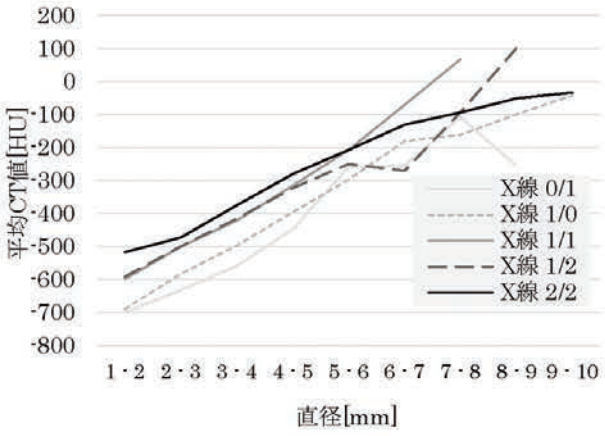

図 4 病型区分別における粒状影の大きさと平均 CT 値

表 1 に CT 画像の粒状影総数に基づいて医師が病型区分を再検討した結果を示す．症例(c)と(e)は CT 画像を用いた定量評価により診断結果が変更されていることが分かる．

表 1 CT 画像の粒状影総数に基づく
病型区分の再検討結果

症例番号	粒状影総数	第1回小症会議での病型区分		再検討後の病型区分	
		①XP合議スコア	②CT合議スコア	③XP合議スコア	④CT合議スコア
(a)	103	0/1	-（アスベスト）	0/1	0/1
(b)	126	0/1	0/1	0/1	0/1
(c)	474	0/1	0/1	0/1	1/0
(d)	260	0/1	0/1	0/1	0/1
(e)	474	0/1	1/0	0/1	1/0
(f)	168	1/0	0/1	0/1	0/1
(g)	237	1/0	0/1	0/1	0/1
(h)	234	1/0	0/1	0/1	0/1
(i)	458	1/0	1/0	1/0	1/0
(j)	577	1/0	4A	4A	4A

4. まとめ

じん肺 CT 画像から粒状影を抽出し，X 線の病型区分に基づいて，CT 画像の粒状影を個数，大きさと CT 値，分布型について解析した．CT 画像を用いた定量評価結果を提示することにより，より正確にじん肺の重症度を分類することが可能となり，診断精度の向上が期待できる．今後の課題として多症例に適用し，より正確なじん肺 CT 画像データベースの作成と高精度な粒状影自動抽出法について検討する．

文　献

[1] H. Suzuki, Y. Kawata, N. Niki, et al: Computer aided diagnosis for severity assessment of pneumoconiosis using CT images, Proc. SPIE Medical Imaging, Vol.9785, pp.978531-1-6, 2016.

[2] K. Kanazawa, Y. Kawata, N. Niki, et al: Computer-aided diagnosis for pulmonary nodules based on helical CT images, Comput. Med. Imag. Graphics, vol. 22, no. 2, pp. 157–167, 1998.

[3] Y. Kawata, N. Niki, H. Ohmatsu, et al: Quantitative classification based on CT histogram analysis of non-small cell lung cancer: Correlation with histopathological characteristics and recurrence-free survival, Medical Physics, vol.39, no.2, pp.988-1000, 2012.

[4] 松廣幹雄，鈴木秀宣，河田佳樹，他：胸部マルチスライス CT 画像における葉間裂抽出法，電子情報通信学会論文誌，Vol.J.96-D, no.4, pp.834-843, April，2013.

[5] 滝島任，中村雅夫，千代谷慶三：じん肺患者の呼吸機能検査ハンドブック．真興交易医書出版部，1991，P3-10

[6] 永井厚志編：呼吸器疾患　第 3 版．日本医事新報社，2015，P241-250

[7] K. Hino, M. Matsuhiro, H. Suzuki, et al: Quantitative assessment for pneumoconiosis severity diagnosis using 3D CT images, Proc. SPIE Medical Imaging, Vol.10575, pp.105753J-1-6, 2018.